model Hamiltonian:

$$H_M'=\sum_i T_i+\sum_i \tfrac{1}{2}M\omega^2 x_i^2+\sum_i U_i, \quad (6)$$

where the modified single-particle potential U_i is related to the modified two-body interaction u_{ij} in the same manner as V_i is related to v_{ij} in the usual treatment. The correspondence between Eqs. (1) and (2) on the one hand and Eqs. (4) and (6) on the other can be shown formally by writing

$$T_i'=T_i+\tfrac{1}{2}M\omega^2 x_i^2. \quad (7)$$

Equations (4) and (6) are then obtained from Eqs. (1) and (2) simply by replacing T_i by T_i', v_{ij} by u_{ij}, and V_i by U_i. Since the usual manipulations of Brueckner theory in a finite nucleus do not require explicitly that T_i be the kinetic energy operator, the same manipulations can be done with T_i'. Therefore all the formal treatment of Brueckner theory can be applied to Eqs. (4) and (6).

In conclusion, we can say that Eqs. (4) and (6) present a modified point of departure for Brueckner theory, with the following differences from the usual treatment:

1. There should be fewer convergence difficulties due to center-of-mass motion.
2. A harmonic oscillator shell-model potential appears in the Hamiltonian *from the beginning* before any approximations are made. It is only the deviation of the shell-model potential from the harmonic oscillator which appears in the perturbation treatment. This seems to be reasonable, since the harmonic oscillator potential has been used widely with good results in practical shell-model calculations.
3. The modified interaction u_{ij} is not a short-range interaction because of the term $(x_i-x_j)^2$. This may cause difficulty if short-range approximations are desirable in calculations.

PHYSICAL REVIEW VOLUME 109, NUMBER 6 MARCH 15, 1958

Angular Distribution of Photoprotons from Deuterium from 9 to 23 Mev*

A. WHETSTONE AND J. HALPERN
University of Pennsylvania, Philadelphia, Pennsylvania
(Received November 19, 1957)

Photoprotons from a deuterated paraffin target irradiated with betatron x-rays have been detected with a NaI(Tl) scintillator. The angle and energy of the protons have been measured, and the data has been fitted to the angular distribution form $f(\theta)=(A+B\sin^2\theta)(1+2\beta\cos\theta)$. The ratio A/B rises from a value of 0.015 ± 0.041 for the 9- to 12-Mev photon group to a value of 0.133 ± 0.020 for the 20- to 23-Mev group. A/B increases in a complicated way suggesting several contributions to the isotropic component. The value determined for β agrees with the calculation of v_p/c. A Schiff thin-target spectrum is assumed for the incident photons, and the cross section obtained is consistent with the Marshall and Guth calculations, although the energy dependence of the data has slightly less slope than the calculated values.

I. INTRODUCTION

THE theoretical calculations[1] of the photodisintegration of the deuteron below photon energies of, say, 25 Mev predict a predominantly $\sin^2\theta$ angular distribution. The electric dipole, ED, transition from the ${}^3S_1$ part of the ground state to the ${}^3P_J$ states accounts for most of the disintegration process. The electric quadrupole absorption causes a fore-aft asymmetry modifying the distribution to $\sin^2\theta(1+2\beta\cos\theta)$. In addition a small isotropic component is predicted, the explanation of which has become one of the most interesting aspects of the deuteron photodisintegration problem at intermediate energies. The usual forms assumed for the angular distribution are

$$f(\theta)=A+B\sin^2\theta(1+2\beta\cos\theta), \quad (1)$$

and

$$f(\theta)=(A+B\sin^2\theta)(1+2\beta_1\cos\theta). \quad (2)$$

The recent experimental determinations of the angular distribution, that of Halpern and Weinstock[2] and that of Allen,[3] have shown the isotropic component in the region of 20 Mev to be considerably larger than that predicted by most of the theoretical work. Experimentally the ratio A/B is found to be about one-tenth at this energy. A brief review of the attempts to explain the observed isotropic component follows.

1. A small contribution comes from the magnetic dipole, MD, transition ${}^3S_1\rightarrow{}^1S_0$. Using the usual potentials, Yukawa or Hulthén, this is estimated to contribute 0.01 or 0.02 to the ratio A/B at these energies.[4,5]
2. The ${}^3S\rightarrow{}^3P_J$ transition in the presence of a tensor

* Supported in part by the Air Research and Development Command and by the U. S. Office of Naval Research.
[1] For a comprehensive bibliography of the work see M. Elaine Toms, "Bibliography of Photonuclear Reactions," Naval Research Laboratory (1955, 1956, 1957).
[2] J. Halpern and E. Weinstock, Phys. Rev. **91**, 934 (1953).
[3] L. A. Allen, Jr., Phys. Rev. **98**, 705 (1955).
[4] N. Austern, Phys. Rev. **85**, 283 (1952).
[5] L. Hulthén and B. C. H. Nagel, Phys. Rev. **90**, 62 (1953).

force in the ^3P state has been shown by Austern[4] to contribute to the isotropic component. Iwadare *et al.*,[6] using a very strong tensor force, can account for about half of the experimental value for A/B by this transition.

3. The $^3D \rightarrow {}^3P$ transition in the presence of a tensor potential in the ^3D state has been considered in reference 6. Also this transition has been calculated by Yamaguchi[7] using a nonlocal but separable potential, the value obtained for A/B being about half of the observed value.

4. A highly singular spin-orbit coupling in the ^3P state can provide some contribution at these energies.[4]

5. The MD transition in the presence of a repulsive core in the $^1S_0$ state has been shown[6] to be capable of giving about half of the required value for A/B. The hard core has the effect of pushing the $^1S_0$ wave function outward to increase the overlap with the deuteron ground state wave function. By combining this effect with effect 2, Iwadare *et al.* have obtained enough isotropic component to match the experimental value at 20 Mev.

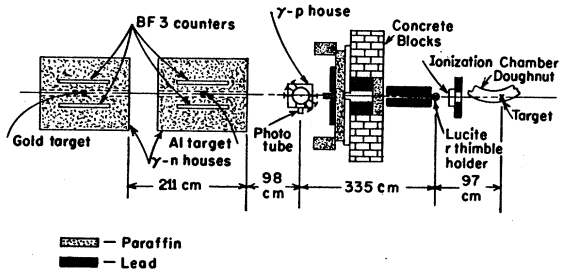

FIG. 1. General arrangement of apparatus.

6. The MD transition can be enhanced by the inclusion of an interaction moment operator. Most investigators[6,8,9] have found this effect to be small but an uncertainty exists.

7. A meson reabsorption model suggested by Whalin, Schriever, and Hanson[10] and by Wilson[11] has been elaborated on by Austern.[12] There is a strong modification of the $^3P_0$ wave amplitude due to a production and reabsorption of virtual mesons. Rather than predicting the isotropic component from the model, Austern has used the existing data to obtain information on this particular electromagnetic interaction.

The present experiment was designed to measure the energy dependence of A/B from 9 Mev to 23 Mev with the idea that a comparison of the data with more detailed calculations of the energy dependence of the above effects could provide a basis for choosing among them. The data have been fitted to forms (1) and (2) so that β and β_1 are determined. Also the total cross section integrated over angles is determined, but the values obtained for σ are subject to the usual uncertainties arising from the difficulty of an absolute determination of the number of photons involved.

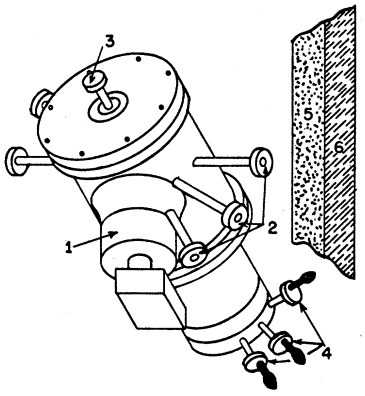

FIG. 2. The target housing. (1) Iron phototube shield; (2) beam ports; (3) target holder shaft; (4) alignment adjustments; (5) paraffin; (6) lead.

II. APPARATUS AND EXPERIMENTAL PROCEDURE

A target of deuterated paraffin, CD_2, was bombarded with the photons produced by the bremsstrahlung of a betatron run at an energy of 23 Mev. The resultant protons were detected by means of a NaI(Tl)scintillator mounted on a photomultiplier tube. The highly collimated beam passes through an aperture in the shielding walls, then through the evacuated (γ,p) house and the two (γ,n) houses. The (γ,p) house is shown in Figs. 2 and 3. There are six beam ports permitting measurements at 30°, 60°, 90°, 120°, 150°, and 270°. The target frame rotates with the entire house so that the target makes a constant angle to the detector. Protons leaving the target lose a small amount of energy which is thus independent of the angle of detection. At 30° and 150° the beam projection on the target is a circle of diameter $\simeq$0.4 in. and at other angles it is an ellipse.

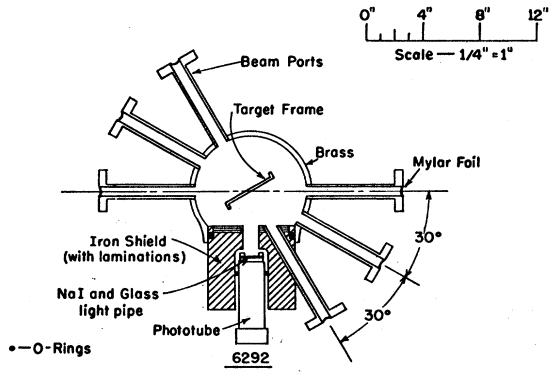

FIG. 3. The target housing, a cross-sectional view from above.

[6] Iwadare, Otsuki, Sano, Takagi, and Watari, Progr. Theoret. Phys. Japan **16**, 658 (1956).
[7] Yoshio Yamaguchi and Yoriko Yamaguchi, Phys. Rev. **95**, 1635 (1954) and Phys. Rev. **98**, 69 (1955).
[8] H. Feshbach and J. Schwinger, Phys. Rev. **84**, 194 (1951).
[9] A. Sugie and S. Yoshida, Progr. Theoret. Phys. Japan **10**, 236 (1953).
[10] Whalin, Schriever, and Hanson, Phys. Rev. **101**, 377 (1956).
[11] R. R. Wilson, Phys. Rev. **104**, 218 (1956).
[12] N. Austern, Phys. Rev. **108**, 973 (1957).

The proton detector measures the energy of the proton and its angle with respect to the beam. These two quantities define the photon energy. The energy resolution of the detector is about 3% for the proton energies encountered in this experiment and about 3.5% for Po^{210} α particles. The detector aperture is a 1-in. diameter circle, and it is 4.64 in. from the axis of the deuterium target. The method of preparing and mounting the scintillator will be described in some detail in a forthcoming paper.[13] The pulses from the photomultiplier tube (DuMont 6292) go through a preamplifier and amplifier (Los Alamos model 100) and are displayed on a 100-channel pulse-height analyzer[14] of the Wilkinson type.

It is necessary to establish the relationship between the pulse height analyzer channel number and photon energy. This is done by getting the $h\nu$ *vs* T_p (proton energy) scale and then the T_p *vs* channel scale. The $h\nu$ *vs* T_p scale comes from the equations for conservation of energy and momentum during the photodisintegration process.[15] These equations were programmed for a Univac computer. Laboratory to center-of-mass angle and solid angle conversions were included in the program. To establish the T_p *vs* channel scale a separate experiment was undertaken in which several well-known (d,p) reactions produced by an electrostatic generator were used as a source of monoenergetic protons. This work will be described in reference 13. Briefly, the (d,p) experiment showed that the proton energy *vs* channel line extrapolated to (0.46±0.10) Mev at channel 0. Brolley and Ribe[16] found this extrapolation to be (0.290±0.005) Mev. The ratio of α to proton energies for registration in the same channel was found to be 1.93±0.04 for 5.3-Mev α particles. The excellent agreement of this ratio with the determination made by Eby and Jentschek[17] would indicate that the disagreement with the extrapolation found by Brolley and Ribe was not due to an unusually poor crystal surface. Referring to Fig. 4, the zero extrapolation and the α-proton ratio give two points on the energy scale.

Background was taken with a CH_2 target, so the maximum energy protons from carbon give a third point on the energy scale. The maximum energy of the protons from deuterium varies with angle giving five additional points on the energy scale. The energies assigned to the carbon and deuterium proton spectrum end points depend on $h\nu_{max}$, the maximum photon energy. For carbon $(T_p)_{max} \sim (11/12)h\nu_{max}$, and for deuterium $(T_p)_{max} \sim \frac{1}{2}h\nu_{max}$. In fitting a line to the eight points the least square sum was minimized with respect to $h\nu_{max}$, and the betatron energy was thus determined to be (22.90±0.05) Mev. The betatron energy was maintained at this value throughout the experiment.

The scintillator was thick enough (≃0.040 in.) to stop the maximum energy protons. For electrons the crystal was thin, so electron pulses were mostly small. A discriminator prevented these from registering on the pulse-height analyzer. Electron pileup (coincidence of small pulses with the larger ones) was virtually eliminated by operating the betatron at low instantaneous intensities but long beam duration (≃100 μsec).

The x-ray beam from the betatron was monitored in several ways. Current from an air ionization chamber was integrated to indicate total photon yield. Next a Victoreen r thimble imbedded in Lucite was inserted into the beam periodically. The two neutron houses shown in Fig. 1 had different targets with different energy responses. The ratio of the neutron yields from these two targets provided a check on energy stability of the betatron (Fig. 5), while the yields themselves constituted a sensitive check of beam intensity. The only beam monitor capable of giving an absolute photon count was the Victoreen r-meter.

It is seen in Fig. 3 that the detector is on one side of the beam at forward angles and on the other at backward angles. Comparison of the 90° and 270° measurements provided a test against any systematic lateral asymmetry. The measurement of A/B is sensitive to geometrical factors, so good resettability was a prime consideration in apparatus design. The proton house is mounted on a milling vise. The angles are measured to an accuracy of one minute, and are resettable to this

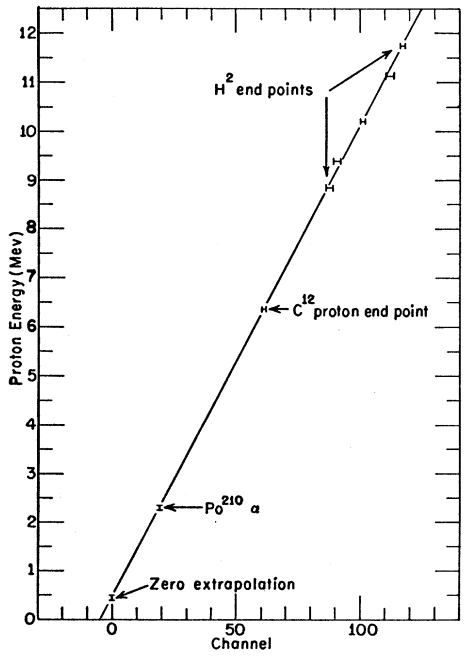

FIG. 4. The proton energy *vs* channel scale. The horizontal errors represent difficulty in assigning a definite channel number to the proton spectrum end points.

[13] Rev. Sci. Instr. (to be published).
[14] R. D. Hiebert *et al.*, Los Alamos Scientific Laboratory Report LA-1565, 1953 (unpublished).
[15] M. Wiener, National Bureau of Standards Circular No. 515 (U. S. Government Printing Office, Washington, D. C., 1951).
[16] J. E. Brolley and F. L. Ribe, Phys. Rev. **98**, 1112 (1955).
[17] F. S. Eby and W. K. Jentschke, Phys. Rev. **96**, 911 (1954).

amount. The axis of the target is determined photographically to be the axis of rotation and to be in the center of the beam. The gain of the phototube and the electronics was checked hourly throughout experimentation by moving a Po^{210} α source into the target position. Linearity of the proton detection electronics was checked regularly with a precision pulser. The proton house and neutron house alignment with respect to the beam was checked photographically at frequent intervals. The relative thickness of the CD_2 and CH_2 targets was determined by setting the detection discriminator to a very low level and counting the pulses due to electrons from the targets. By determining the thickness ratio of the targets as actually mounted in the beam, several possible sources of systematic error in the background subtraction were eliminated.

The CD_2 and CH_2 targets were prepared by pressing the wax between two steel surfaces. At the end of the experiment the targets were carefully cut up and the pieces weighed and measured. Since the beam projection on the target changed from a circle to an ellipse at different angles, the areal densities of the targets had to be accurately determined over the useful areas.

III. THE DATA

The experiment required 1100 hours of betatron time. The total radiation at the target was 5.5×10^5 roentgens with slightly more than half of the total used for CH_2 plus blank background. The data were taken in six individual runs. In the analysis of the data the runs were kept separate up to a point where they could be tested for statistical agreement. The experimental conditions varied in a few details from run to run. Comparison of the runs, then, provided a test against systematic errors arising from these details. It was seen that the six runs satisfied a statistical test in each of the energy intervals. No data were discarded.

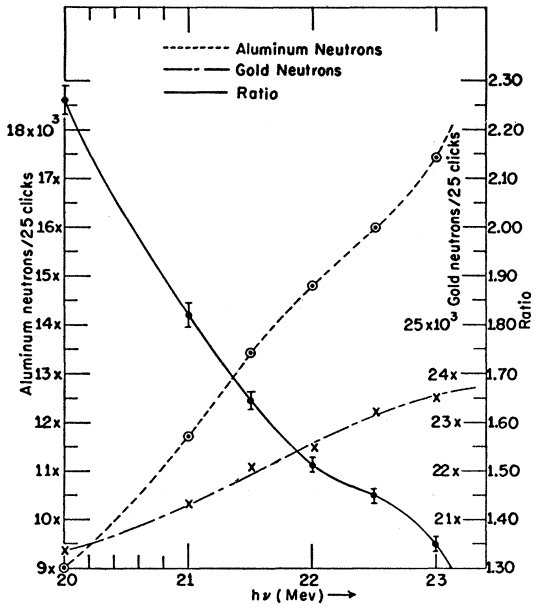

FIG. 5. Counts from the neutron houses. The counts provide a monitor of beam intensity and the ratio of counts provides a sensitive check on energy stability of the betatron.

The protons from carbon and the target electrons are given by CH_2 counts$-$blank counts. The protons from deuterium are given by the counts of

$$CD_2-\frac{N_1}{N_2}f\left[CH_2-\frac{N_2}{N_3}(\text{blank})\right]-\frac{N_1}{N_3}(\text{blank}),$$

where f is the thickness ratio of the CH_2 and CD_2 targets and N_1, N_2, and N_3 are the neutron monitor counts recorded during the CD_2, CH_2, and blank runs, respectively. The neutron counts were taken as the prime beam monitor. These counts agreed with the other monitors to a small fraction of a percent throughout the experiment.

The net deuterium proton counts thus arrived at were next changed, via the energy scale established above, from their channel grouping into photon energy groupings one Mev wide. The data were then corrected for:

(1) Pulse-height analyzer dead time. This was a function of angle and background counting rate.

(2) Irradiation time at each angle related to the irradiation at 90°.

(3) Number of nuclei in the beam as a function of angle.

(4) Detector solid angle which varied from angle to angle as a result of the center-of-mass motion. This correction depended on photon energy.

At this point the six individual determinations were combined. It was not feasible to further process the runs individually because the next phase of the data processing, that of correcting for target absorption, was a tedious reiterative process and it was desirable to do it just once for each angle. The runs were combined with proper weighting for the errors associated with each run.

To correct for proton energy losses in the target, the range energy tables of Rich and Madey[18] were used. By successive approximations a proton spectrum was found, which, when the absorption was applied, produced the observed spectrum. This had to be done at each angle. Figure 6 shows the result for the data taken at 90°. The lower curve is the data corrected for the several effects cited above but not corrected for target absorption. The errors shown are the standard deviations. The target absorption correction produces the upper curve. It is seen that the effect is quite large. It is noteworthy, however, that the result for A/B is almost identical for the corrected and uncorrected data. Thus any small

[18] M. Rich and R. Madey, Atomic Energy Commission Report UCRL-2301, 1954 (unpublished).

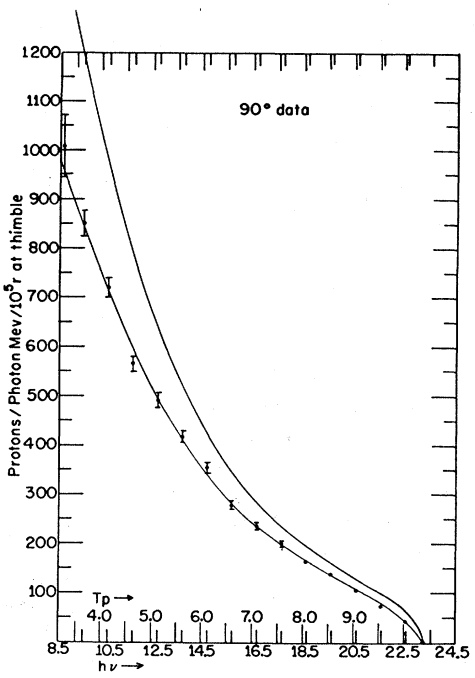

FIG. 6. The 90° data plus the 270° data. The upper curve represents the target absorption correction applied to the data.

uncertainty in the absorption correction produces a negligible error in A/B. For β, β_1, and the total cross-section values, the target absorption correction is important.

The angle designations, 30°, 60°, etc., are nominal. Corrections must be applied for laboratory to center-of-mass coordinate conversion and for the finite extent of the beam on the target and for the finite solid angle of the detector. (This latter correction is small since the detector half-angle is about 6.2°, so it can be applied either as a counting rate change or as an angular change without introducing error of consequence.) These corrections are, of course, different in each photon bin.

The data were next folded about 90° to eliminate β. This had to be done reiteratively because the backward angles were not exactly supplements of the forward angles, so the resultant distribution had to be used to effect the correct folding.

$$G(\theta)=[F(\theta)+F(180-\theta)]/2=A+B\sin^2\theta,$$
$$H(\theta)=[F(\theta)-F(180-\theta)]/4B=\beta\sin^2\theta\cos\theta$$
$$=\beta_1[(A/B)\cos\theta+\cos\theta\sin^2\theta].$$

$G(\theta)$ is plotted against $\sin^2\theta$ so that the intercept with the abscissa gives A/B independent of β. The slope of $H(\theta)$ *vs* $\sin^2\theta\cos\theta$ gives β subject to the previous determination of B, and the slope of $H(\theta)$ *vs* $[(A/B)\cos\theta+\cos\theta\sin^2\theta]$ gives β_1 subject to previous determination of A and B. These plots were fitted by the weighted least-squares method in each photon bin from 9 Mev to 23 Mev. The errors on A/B, β, and β_1 can be calculated in two ways: first, by differentiating the least-squares formulas, putting in the standard deviation of the data for the increments, and combining the contributions quadratically, and second, by observing the deviations of the data points from the least-squares lines. When these methods are compared for all of the energy bins it is seen that the second method gives the smaller error in most cases. In fact, the errors by the two methods are in a ratio of 1.6:1 considering all energies. The reason for this can be seen by referring to Fig. 6. The data points have been connected by smooth lines to facilitate the application of the target absorption corrections. If the bremsstrahlung energy dependence and the deuteron photodisintegration energy dependence are assumed to be smooth, then the data in each energy bin is effectively improved by connecting the data points by a smooth curve. For this reason the points of the $F(\theta)$ plot lie closer to the line than would be expected statistically. The second method of computing the error cannot be used for each energy bin because, with so few points on the line, the result can be accidentally too good or too bad to be realistic. The first method has been used, but the result for each bin has been divided by 1.6 as indicated by comparison of the two methods over all energy bins. The improvement in the results comes about from adding information to the data, i.e., knowledge of the smoothness of the bremsstrahlung and photodisintegration processes, at least over energy intervals a few Mev wide.

There are several possible sources of systematic error in A/B. First the background subtraction is quite large at 9 Mev, so any uncertainty in the target thick-

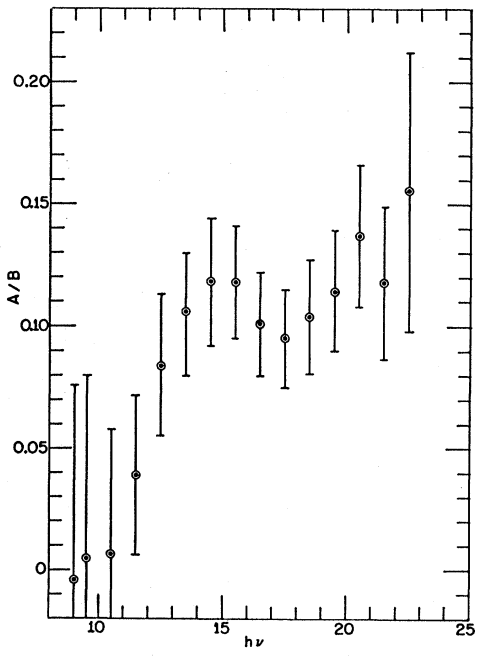

FIG. 7. A/B *vs* energy. The errors shown are the standard deviation plus systematic errors combined additively.

ness ratio becomes important. Above 15 Mev there is no background. This error in A/B is 0.02 at 9 Mev and decreases rapidly to zero at 15 Mev. The initial measurement of the angles was made to 0.05°. The resettability error is a like amount. The error introduced in A/B is 0.002. The target uniformity has been indicated to be of importance; 0.002 is the error assigned to A/B as a result of the correction for nonuniformity. As the (γ,p) house is rotated there is the possibility of a slight change of detector solid angle arising from several possible geometric considerations. The resultant error in A/B is taken to be 0.001. These errors have been included additively in the total errors presented for A/B. No error is considered to arise from the energy scale of the detector, from shift of peak energy of the betatron, or from the calculations. There are other sources of errors which affect β and the cross section but not A/B.

The resulting values for A/B are presented in Fig. 7. Figure 8 shows the results for A/B when the data are put into larger energy bins. β and β_1 are shown in Fig. 9 together with the curve of v_p/c *vs* photon energy.

To calculate the cross section as a function of photon energy from the data, it is necessary to make an assumption about the photon spectrum. For this work the Schiff thin-target forward spectrum[19] is used. The spectrum is modified for small amounts of absorbing material between the betatron target and the Lucite block which holds the r thimble. The total energy incident on the Lucite block is converted into esu following the method of Zendle *et al.*[20] Figure 6 of this reference gives the calculated conversion from ergs to esu. Laughlin *et al.*[21] have made a calorimetric determination of the conversion for a betatron peak energy of 22.5 Mev, the result of which is included in Fig. 6 of Zendle *et al.* The conversion read from this figure for 23-Mev peak energy is 5720 ergs cc/esu cm^2. The energy in each Mev bin is divided by the mean photon energy to obtain the number of photons/cm^2-Mev. Further corrections are made for air and other materials between the r-thimble location and the CD_2 target. The resultant spectrum is applied to the data in order to compute the cross section. The results are shown in Fig. 10. The solid curve represents the Marshall and Guth[22] calculation for 50% exchange in the proton-neutron interaction.

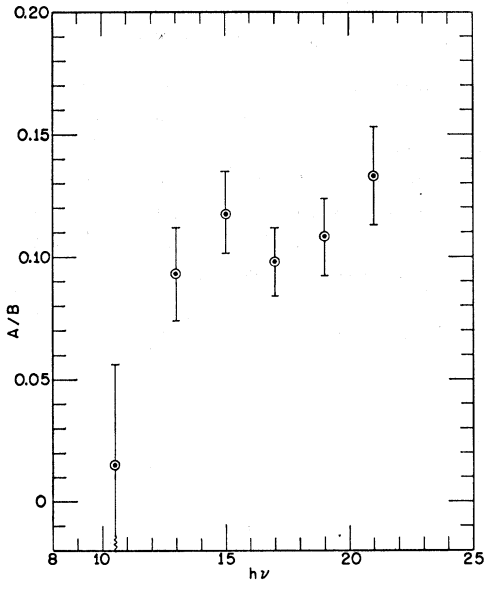

FIG. 8. A/B *vs* energy. The energy bins are larger than those of Fig. 7.

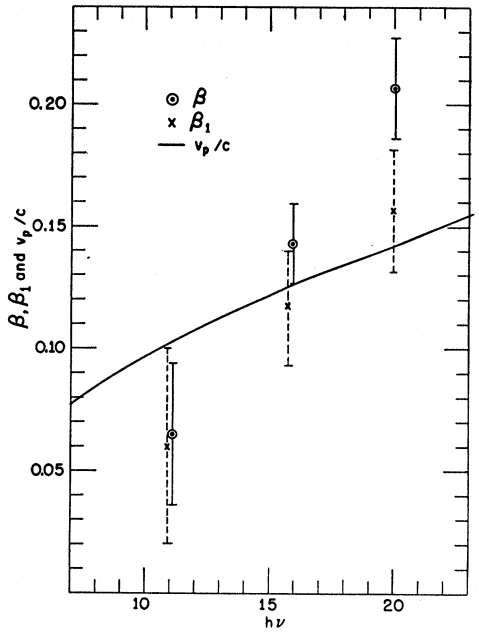

FIG. 9. β and β_1 are determined by fitting the data to Eqs. (1) and (2) after a previous determination of A/B. The errors shown are statistical plus systematic. For comparison the function v_p/c is plotted.

Errors which affect the total cross-section results but not the angular distribution results are listed below.

1. The shape of the bremsstrahlung spectrum used. No error has been included in the presentation of the cross section, Fig. 10, due to this source of uncertainty. If one wishes to assume the slope of the Marshall-Guth calculation to be substantially correct, then the trend of the data points would suggest a spectrum with more photons at the high end than the one used.

2. r-thimble calibration. The thimble used has a capacity of 250 r. It was calibrated by comparison with a 100-r thimble which has been calibrated by the National Bureau of Standards. A Landswerk r thimble and Lucite block at a different location in the laboratory

[19] L. I. Schiff, Phys. Rev. **83**, 252 (1951).
[20] Zendle, Koch, McElhinney, and Boag, Radiation Research **5**, 107 (1956).
[21] J. S. Laughlin *et al.*, Am. J. Roentgenol Radium Therapy Nuclear Med. **70**, 294 (1953).
[22] J. F. Marshall and E. Guth, Phys. Rev. **78**, 738 (1950).

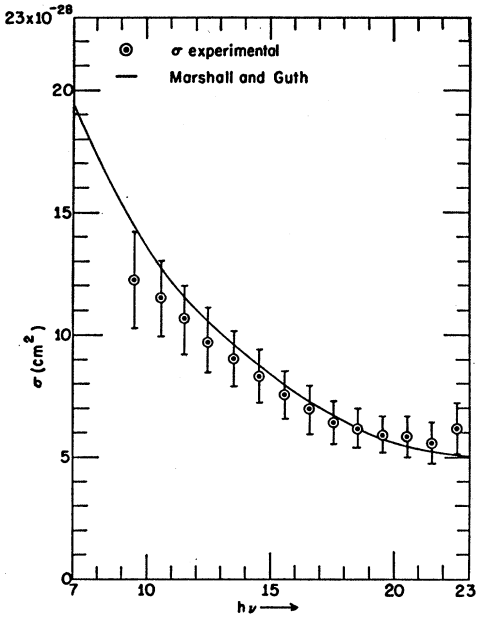

FIG. 10. The solid curve is the Marshall-Guth calculation for 50% exchange. The Schiff bremsstrahlung spectrum is used with the data to obtain the experimental points. The error indicated is largely systematic and is due to the difficulty of ascertaining the uumber of photons involved.

gave results in agreement with the Victoreen instrument to about 1%. An error of 5% is assigned to the calibration because of indirectness of the comparisons.

3. The error indicated for the calorimetric measurement of Laughlin *et al.* is about 5% and this error is included in the present work.

4. There are numerous sources of small errors in the measurements of the geometry of the experiment.

The errors of item 4 and the previously discussed errors which contribute to A/B are combined quadratically with the counting statistics. The contributions of items 2 and 3 total 10% and this amount is included additively in each energy bin. The resulting errors are shown in Fig. 10. It can be judged from the scatter of the points that the statistical errors are smaller than the systematic ones. For this reason there is nothing to be gained by grouping the data into larger energy bins.

IV. DISCUSSION

For the photon group 20 to 23 Mev the present experiment finds $A/B=0.13\pm0.02$. Allen has obtained a value of 0.11 ± 0.01 for the 20- to 25-Mev group. Halpern and Weinstock obtained 0.13 ± 0.04 for photons between 18 and 22 Mev. These values can be considered to be in good agreement. At the lower photon energies, 9 to 18 Mev, there is very little previous work of sufficient accuracy to invite comparison. A measurement was made by Fuller[23] with a 20-Mev betatron as a photon source and photographic plates as the proton detectors. Although the accuracy is low because of insufficient data, the results are consistent with those of the present paper.

It does not seem possible to connect the A/B values, Fig. 7, with an uninflected curve. The points do not appear to scatter as much as the assigned error would indicate they should. The reason is that the data are smoothed somewhat for the target absorption correction, so that the value for A/B in a given energy bin does not scatter much from its neighbors. No error which extends over several Mev can be introduced in this way. To connect the data with an uninflected curve, too many adjacent points would be forced to lie above or below the curve. It is concluded, then, that the isotropic component increases in two stages; the first increase starting around 10 or 11 Mev and the second around 18 or 19 Mev. The slope of a line fitted to the six highest points satisfactorily matches the slope of Allen's data, which extend up to 65 Mev. This two-stage effect is suggestive of two or more sources of the isotropic component.

ACKNOWLEDGMENTS

The authors wish to express their gratitude to Dr. P. Yergin, for his help with the apparatus and the targets, to Dr. E. G. Muirhead for many enlightening discussions, to Dr. B. Cook for preparing the Univac program, to Mr. Allison and Mr. Geller for operating the betatron and recording the data, and to Mr. Raje and Mr. Jain for data processing.

[23] E. G. Fuller, Phys. Rev. **79**, 303 (1950).